UNCLASSIFIED

Defense Technical Information Center
Compilation Part Notice

ADP012364

TITLE: Modeling of Mascotte 10 Bar Case with Thesee Code with and without a Secondary Atomization Model

DISTRIBUTION: Approved for public release, distribution unlimited

This paper is part of the following report:

TITLE: 2nd International Workshop on Rocket Combustion Modeling: Atomization, Combustion and Heat Transfer held in Lampoldshausen, Germany on 25-27 Mar 2001

To order the complete compilation report, use: ADA402618

The component part is provided here to allow users access to individually authored sections of proceedings, annals, symposia, etc. However, the component should be considered within the context of the overall compilation report and not as a stand-alone technical report.

The following component part numbers comprise the compilation report:
ADP012355 thru ADP012373

UNCLASSIFIED

MODELING OF MASCOTTE 10 BAR CASE WITH THESEE CODE WITH AND WITHOUT A SECONDARY ATOMIZATION MODEL

Emmanuel Bodèle, Iskender Gökalp
Centre National de la Recherche Scientifique
Laboratoire de Combustion et Systèmes Réactifs
1c Avenue de la Recherche Scientifique
45071 Orléans Cedex 2 France

Stephan Zurbach, Didier Saucereau
SNECMA Moteurs
Groupe SNECMA
BP 802 Forêt de Vernon
27208 Vernon France

Introduction

This paper presents the results of numerical simulations corresponding to the MASCOTTE 10 bar case, done by LCSR and SNECMA. These computation concern mainly the comparison between two cases : one case with a secondary atomization model developed at LCSR and one case without secondary atomization. In this paper we will describe shortly the secondary atomization model (other details are available in ref. [1,2]), the operating point (condition of injection, computational domain, ...), and finally we will discussed briefly the main results issuing of these computations.

The secondary atomization model

The secondary atomization model is based on an experimental study which concerns the characterisation of the secondary break-up process in terms of break-up regimes, characteristic times and secondary distributions (for mores details see ref. [3]).
The break-up regime is determine with the following correlation:

$$\frac{We}{\sqrt{Re}} = C.DR^{0.25}.VR^{-0.5}$$

Where DR and VR represent respectively the density en viscosity ratios between the gaseous and liquid phases. The value of the constant C determine the transition between the 3 break-up regimes considered in this study: 0.25 for bag break-up, 0.7 for transitional break-up and 0.9 for shear break-up.

When a droplet is in one of these 3 break-up regimes, i.e. C greater than 0.25, an evaluation of the duration for the break-up time called initiation time T_{ini} is done with the relation:

$$T_{ini} = 0.75\ T\ We^{-0.06} \quad where \quad T = \frac{D_0}{V}\sqrt{\frac{\rho_l}{\rho_g}}$$

Finally, after a duration equal to Tini, the break-up occurs, and the initial droplet is decomposed in secondary fragments following a distribution in size and number, as shown in the table below:

	Size of secondary fragments (fraction of initial droplet diameter)			
Break-up regime	**10%**	**30%**	**50%**	**Residual**
Bag break-up	2	2	1	93,60%
Transitional Break-up	3	1	1	94,50%
Shear Break-up	2	4	2	86,20%

Operating point

The specification for the MASCOTTE 10 bar case are respectively 10 bar, 2.11, 50g/s and 23.7g/s for pressure, mixture ratio, mass flow rate of liquid oxygen and mass flow rate of gaseous hydrogen. Liquid oxygen is introduce in the computational domain with a Rosin Rammler distribution with D_{32}=82µm at the surface of a liquid core as shown in figures 1 and 2 .

Computational domain and liquid oxygen injection

The computational domain consists in a 2D axisymetric geometry (fig. 1). The domain is 400 mm long and 28 mm for radius. The nozzle is not modelled. Droplets are introduced in the computational domain with a constant normal velocity (fig.2).

Overview of the THESEE code and condition of simulation

The code used for these computations is the THESEE code operated by SNECMA. This solver can operate with 2D or 3D configurations, multiphase, multispecies turbulent reactive flows.

The computations are performed with the following properties:

- Compressible reactive flow
- K-e turbulence model
- EBU combustion model
- Sirignano-Delplanque vaporization model
- Variable thermodynamic properties for the liquid oxygen
- Ideal gas law and variable thermodynamic for hydrogen

In the computational domain, four species (3 gaseous and 1 liquid) are considered : gaseous hydrogen (GH_2), gaseous oxygen (GO_2) obtain by vaporization of liquid oxygen (LOX) and gaseous water (H_2O). A single chemical reaction is used to obtain H_2O from gaseous hydrogen and gaseous oxygen:

$$H_2 + \frac{1}{2}O_2 \rightarrow \text{Products}(H_2O + \text{Dissociation})$$

The Cv for H_2O is corrected to take into account the dissociation processes of water at high temperature. All the properties for liquid and gaseous phases are function of temperature.

Numerical results

The results presented in this part are essentially a comparison between the case with the secondary atomization model activated and the case without the secondary atomization model. The total CPU time to obtain all these results is about 300 hours

Mass fraction contours

On figures 3 and 4 are represented the mass fraction for the 3 gaseous species present in the computational domain. With these figures is it easy to see the apparition of gaseous oxygen near of the liquid injection zone due to the vaporization and the rapid disappearing of the gaseous oxygen and appearing of gaseous water due to the combustion process.

The reaction rate

On figures 5 and 6 the reaction rate is represented for the two cases of computation. In these figures it is clear that the flame form is directly influenced by the secondary atomization process. The thickness of the flame is higher in the case of computation without secondary atomization model because of the bigger droplet and therefore because of the difference of the

vaporization times in these two cases of computation. The flame is positioning nearer of the liquid injection zone in the case of computation with the secondary atomization model activated.

Radial profiles of mean temperature

On figures 7 and 8 radial profiles of mean temperature are represented for several axial locations. For the two cases of computation, the maximal temperature is obtain for the X/D1=10 location, with a maximal temperature of about 3000K.

Axial profiles of mean temperature

On figure 9 and 10, axial profiles of mean temperature are represented for 4 radial locations. The maximal temperature is obtain for the Y/D1=2 location, with a maximal temperature of about 3200K. the oscillation of mean temperature for computation with the secondary atomization model at the X/d1=3 and X/D1=4 locations are due to a divergence of computation during the simulation.

The field of temperature

The figures 11 and 12 are representation of the field of temperature for the two cases of computation. With these two figures it is not easy to characterise the difference between the two cases of computation.

Droplet location

The figures 13 and 14 are representation of superimposition of mean velocity field and droplets in the two cases of computation. The first remark with these two figure is the difference of size for the droplets in the two cases of computation and the efficiency of the secondary atomization process. Secondly, the length of the "spray" is higher in the case of computation without the secondary atomization model because of the slower vaporization of big droplets.

Conclusion

A secondary atomization model has been developed and used to simulate the MASCOTTE 10 bar case. Results presented here show the difference between two cases of computation which correspond to a calculation with the break-up model activated and a case without the break-up model.

The main difference between these computations appears on the flame structure : location, length and thickness. Another difference is the liquid location in the computational domain : there is no more droplets in the computational domain after a distance of about 4 cm from the injection when the secondary atomization model is activated whereas in the other case, droplets already exist up to 10 cm.

References

[1] Gökalp, I, Cousty, R., Vieille, B., Bodèle, E., Fedioun, I., Saucereau, D. and Zurbach, S., *AIAA paper n°2000-3946*, (2000).

[2] Gökalp, I, Bodèle, E., Cousty, R., Vieille, B., Fedioun, I., Saucereau, D. and Zurbach, *Proceedings of the 6th French-German Colloquium on Research in Liquid Rocket Propulsion*, (2000).

[3] Vieille, B., *PhD Thesis, University of Orléans*, France, (1998).

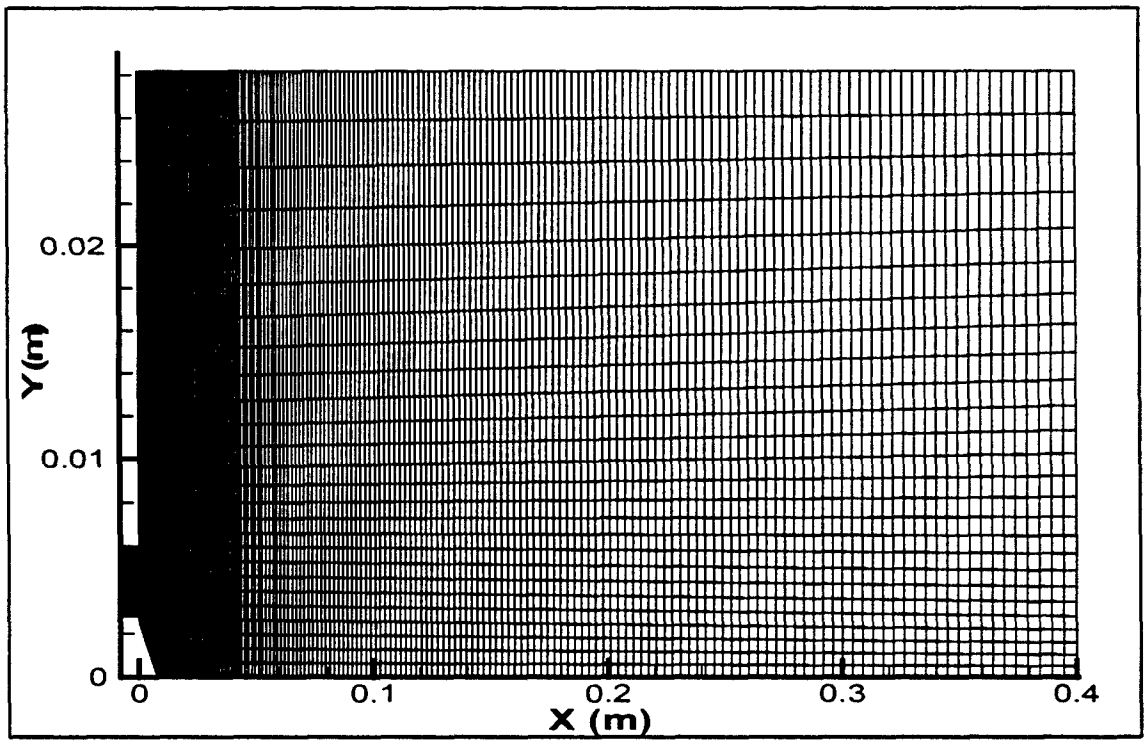

Figure 1. The computational domain

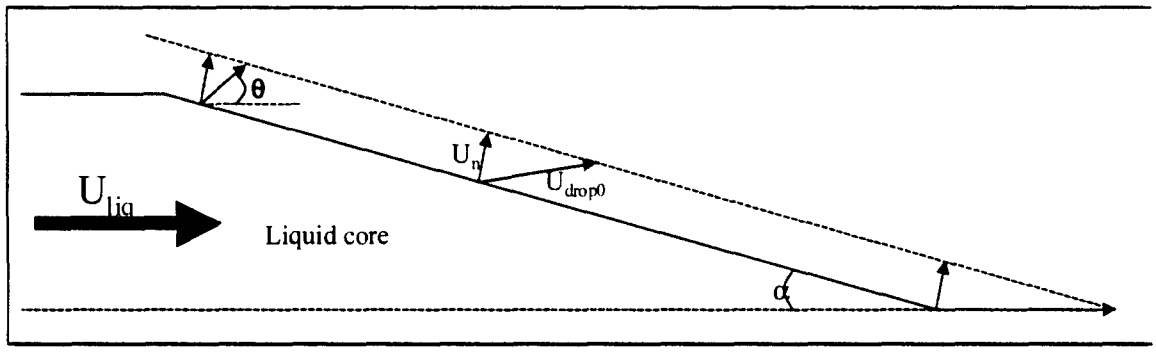

Figure 2. Injection of droplets

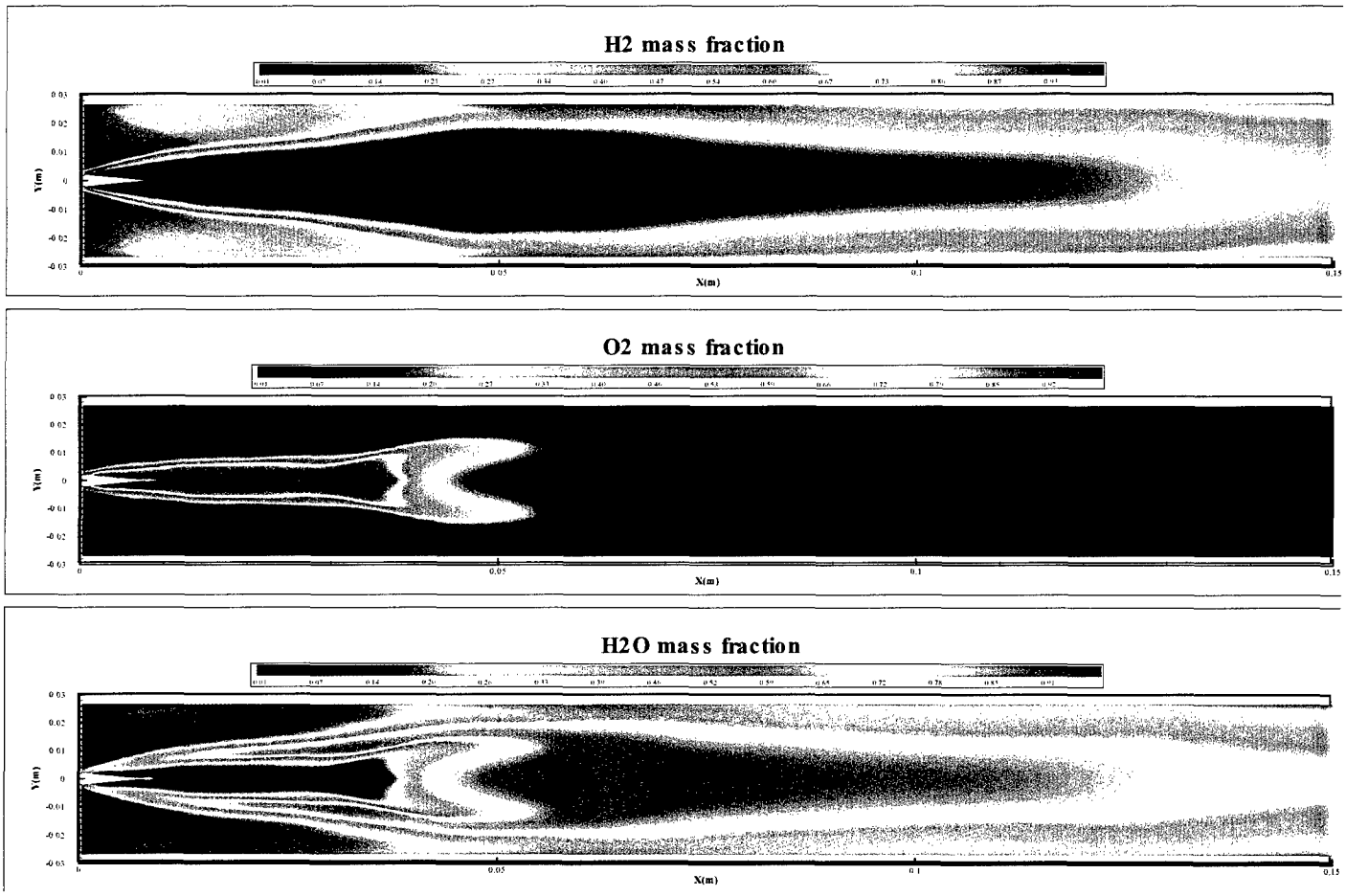

Figure 3. Mass fraction for computation with secondary atomization

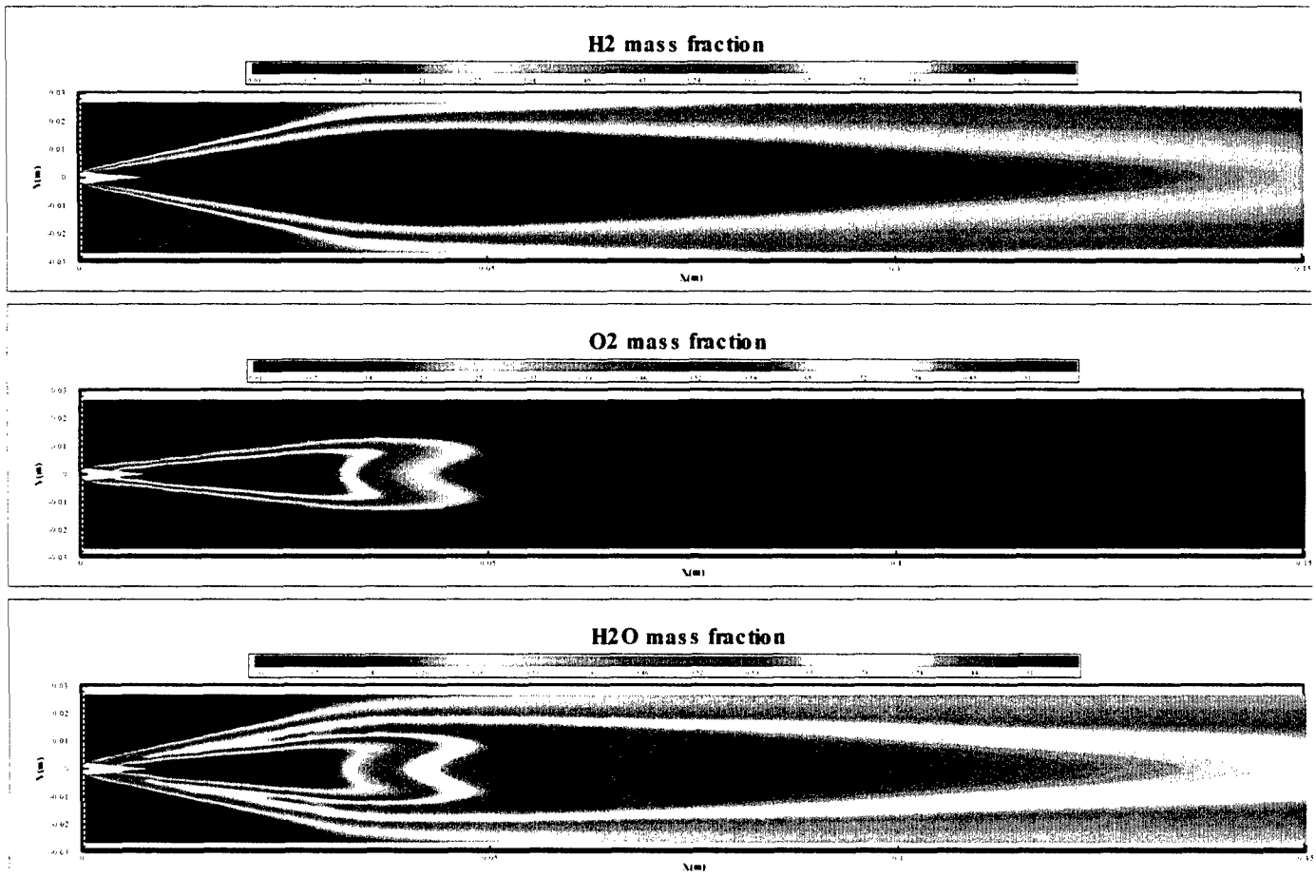

Figure 4. Mass fraction for computation without secondary atomization

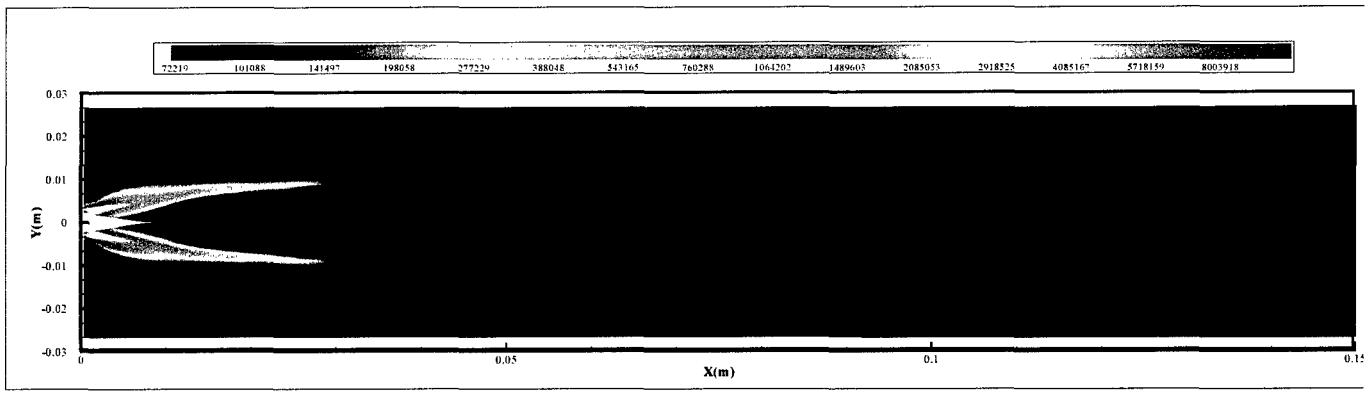

Figure 5. Reaction rate for computation with secondary atomization

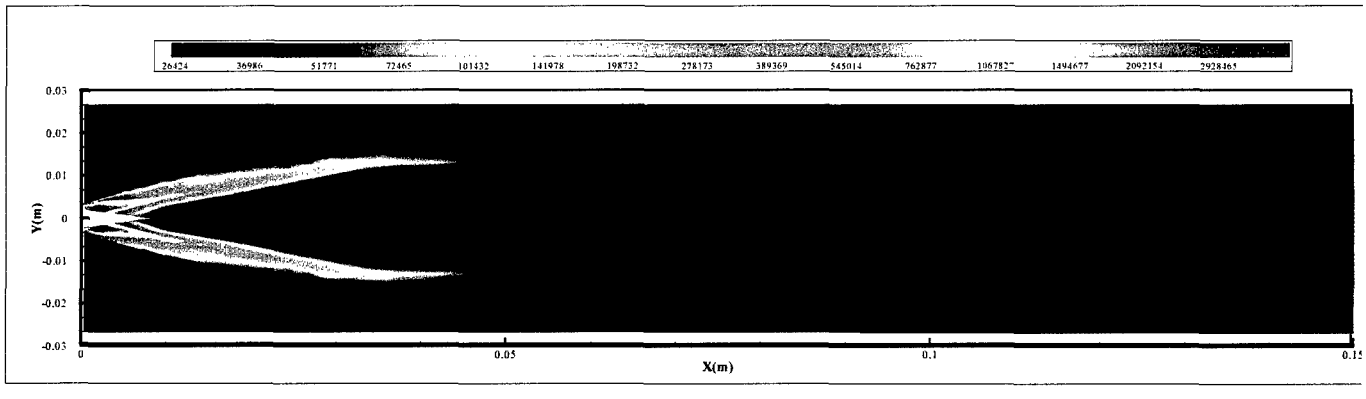

Figure 6. Reaction rate for computation without secondary atomization

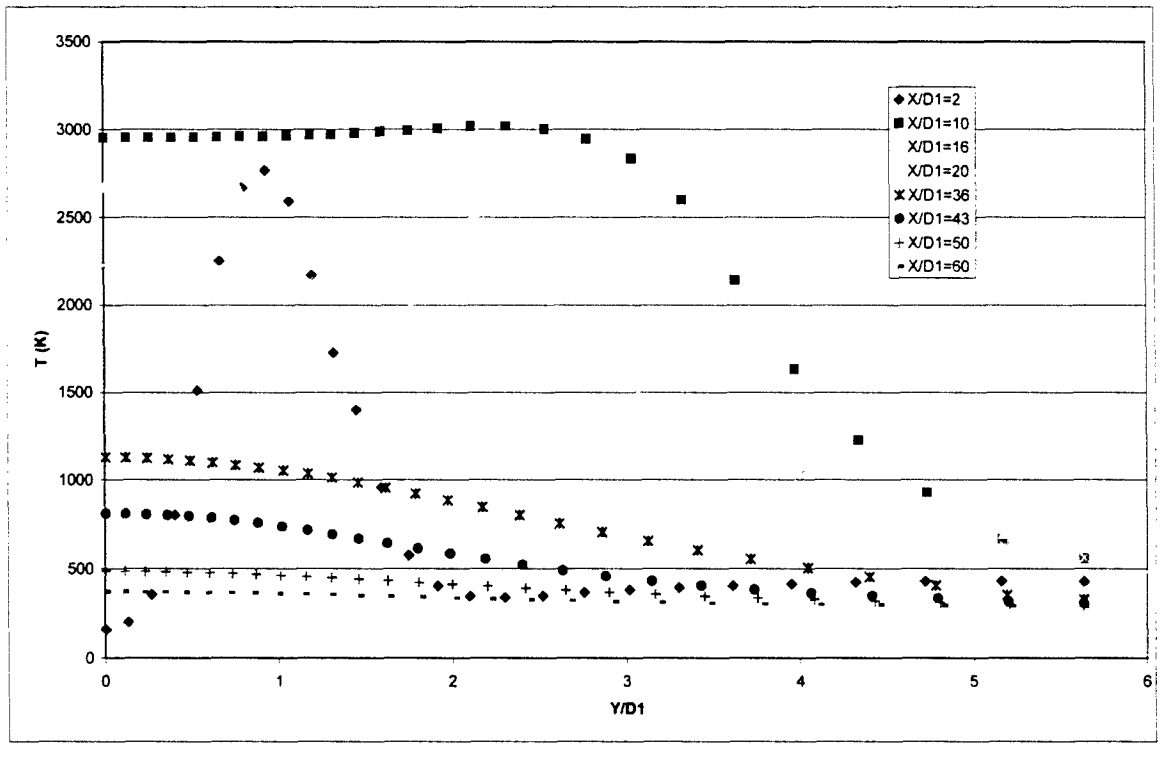

Figure 7. Radial profiles of mean temperature for computation with secondary atomization

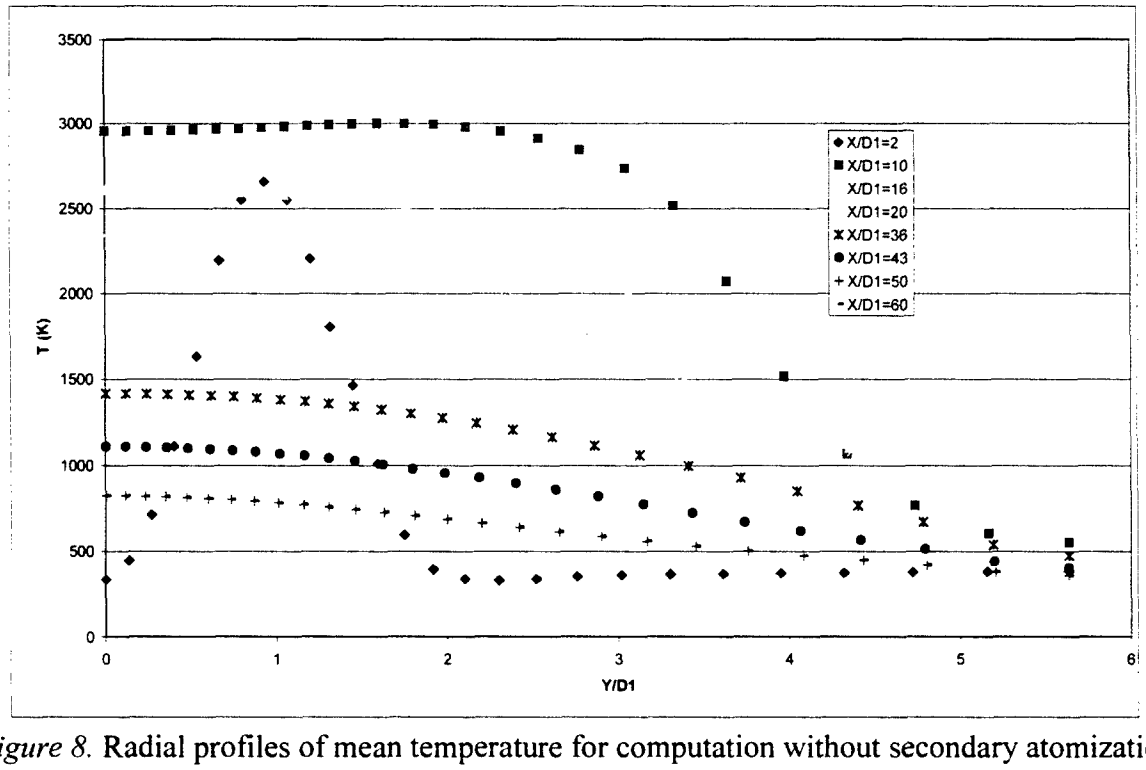

Figure 8. Radial profiles of mean temperature for computation without secondary atomization

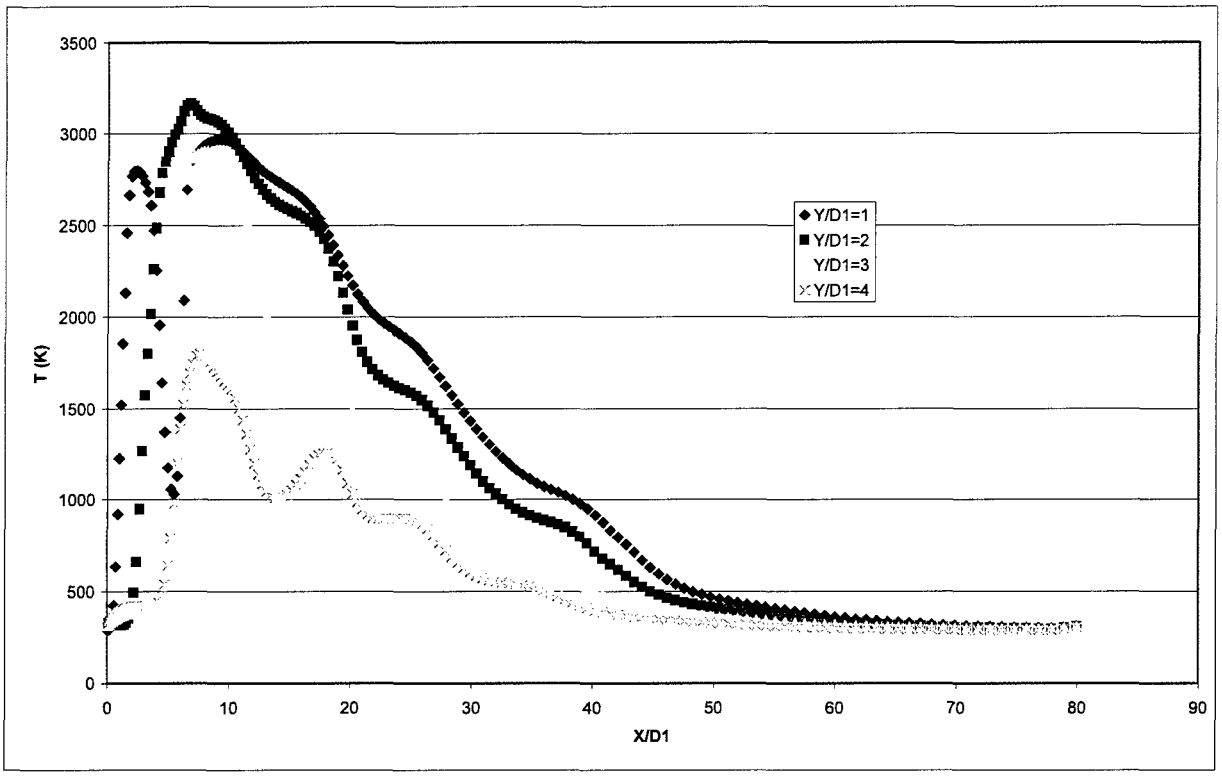

Figure 9. Axial profiles of mean temperature for computation with secondary atomization

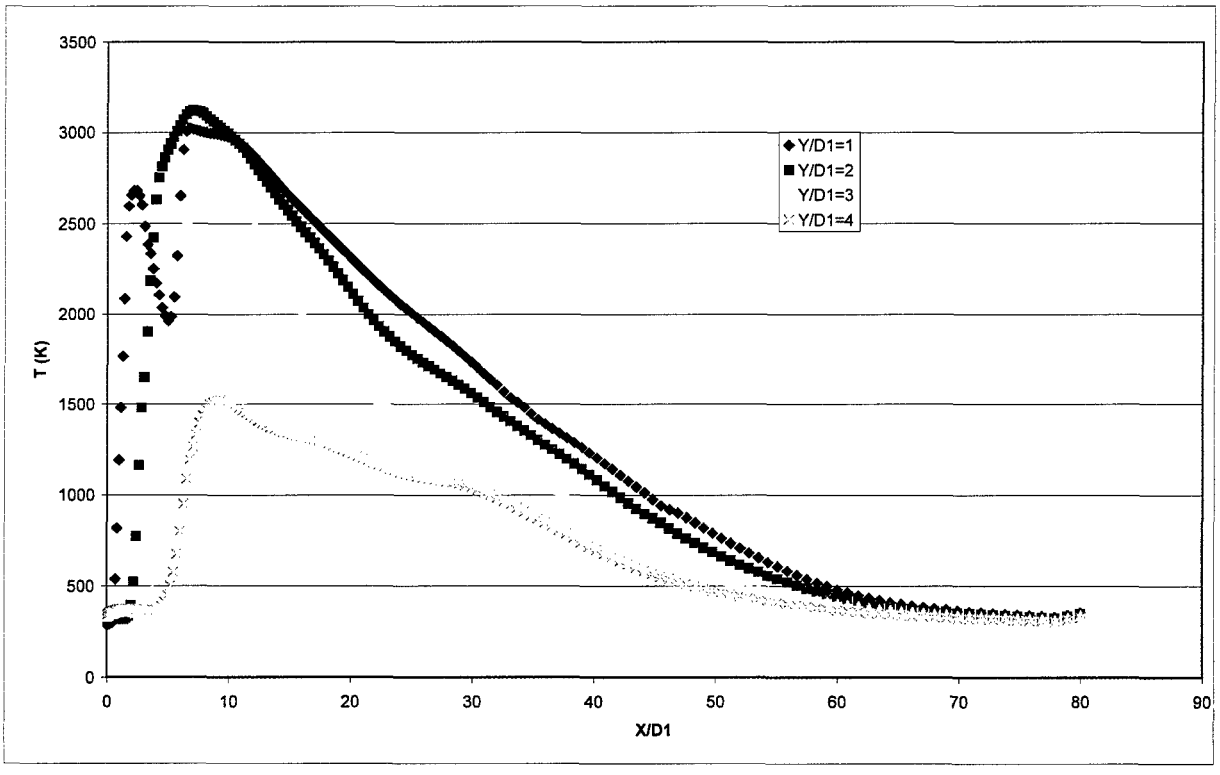

Figure 10. Axial profiles of mean temperature for computation without secondary atomization

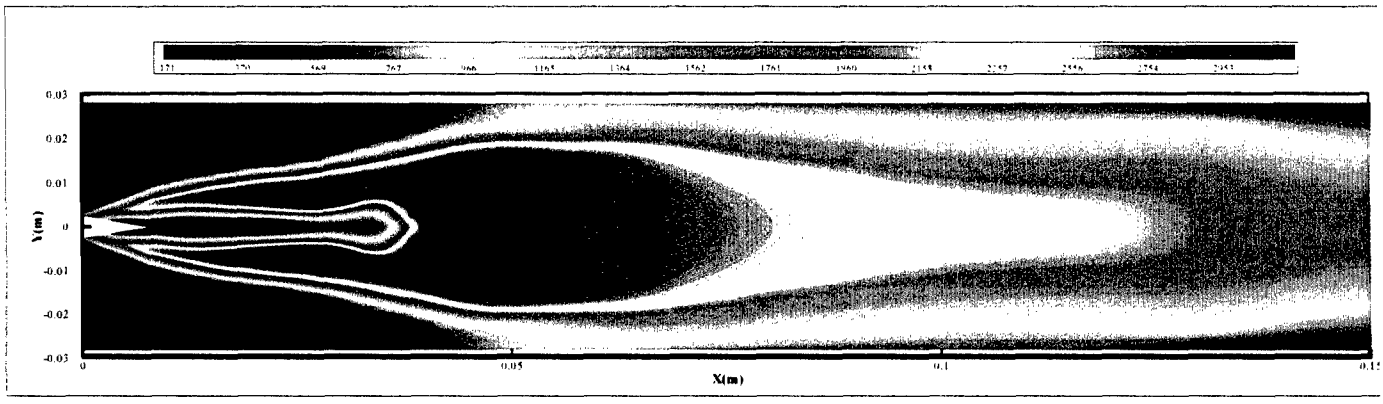

Figure 11. Field of mean temperature for computation with secondary atomization

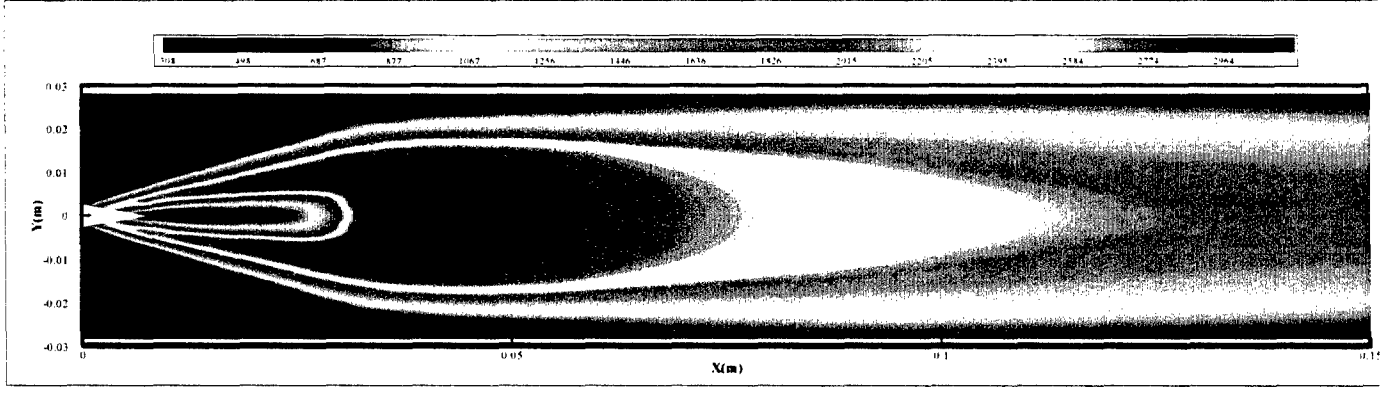

Figure 12. Field of mean temperature for computation without secondary atomization

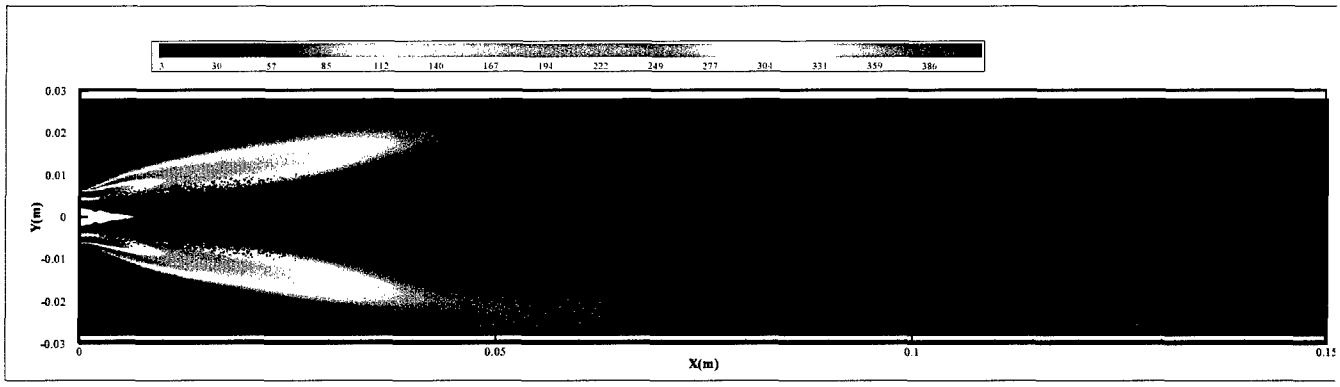

Figure 13. Superimposition of mean velocity field and droplets for computation with secondary atomization

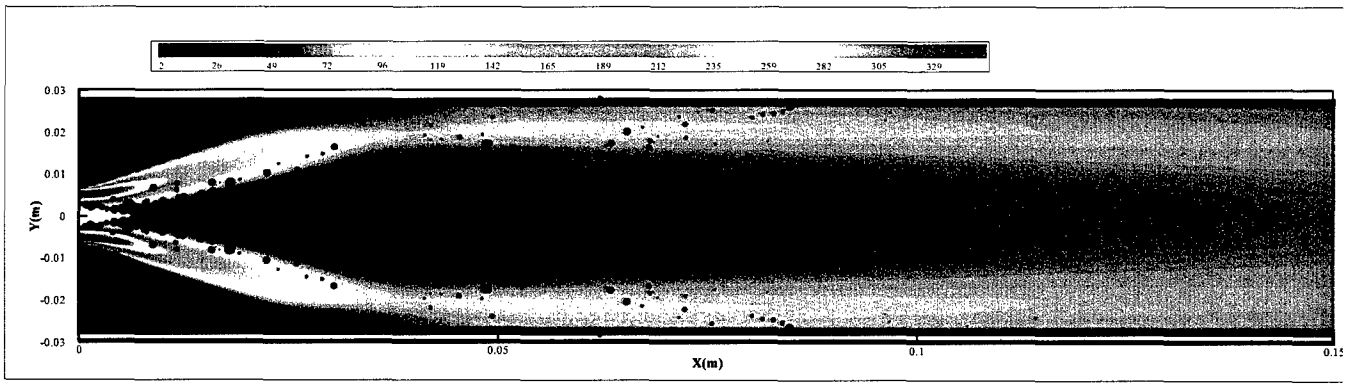

Figure 14. Superimposition of mean velocity field and droplets for computation without secondary atomization